15TH IEA HEAT PUMP CONFERENCE
MAY 26–29, 2026 | HOFBURG
VIENNA 2026
DECARBONISATION THROUGH INNOVATION

# Matching heat pump technologies with process requirements: A heat pump integration framework

Florian Schlosser[a,*], Stephen Braun[a], Henning Meschede[a]

[a]Department of Energy System Technologies, Paderborn University, Warbuger Str. 100, 33098 Paderborn, Germany

**Abstract**

Industrial process heat in the temperature range up to 200 °C accounts for around 40% of industrial final energy demand. The heat pump is a core technology for decarbonisation thanks to its Coefficient of Performance (COP) > 1. A large-scale market ramp-up is currently still being prevented by a lack of knowledge of sensible application options and a lack of standardisation. This paper presents a novel integration framework that characterises and classifies process requirements and matches them with technological concepts and their application limits and efficiencies in order to make recommendations for meaningful integration concepts. On the one hand, the method relies on thermodynamic modelling and uses pinch analysis approaches to describe the process requirements. On the other hand, the application areas and efficiencies of the heat pump technologies are modelled. A targeting algorithm scans the modelled requirements and provides technological recommendations and COPs for various areas of application - classified according to temperatures, media, temporal production behaviour and unit operations. The results are integration concepts for clusters of processes with similar requirements, such as drying, the thermal activation of solid and fluid products, and thermal separation. Suitable integration points and COP estimates are provided for various heat pump technologies.



*Keywords: Process Integration; Pinch Analysis; High-Temperature Heat Pumps, Energy Demand Modelling*

## 1. Introduction

Increasing energy costs, reliance on fossil fuels and growing pressure on reducing carbon footprints are driving companies to explore decarbonization strategies for process heat. Among these, heat pumps utilizing renewable electricity to upgrade waste heat, offer an energy-efficient alternative to traditional heating methods. Technologies on different levels of maturity are capable of reaching up to 200 °C and beyond [1]. This makes them adaptable to a range of industrial processes. For temperatures below 100 °C the effectiveness of industrial heat pump applications has already been well established with 155 demonstration cases in the Annex 48 [2].The temperature range between 100 °C and 200 °C accounts for 26% of industrial process heat, which is still predominantly supplied by fossil fuels [3]. The market uptake of High-temperature Heat Pumps (HTHP) supplying temperatures above 100 °C remains limited. Only 40 demonstration cases in the range from 100 °C to 300 °C could be documented [1]. The economic feasibility is limited by the COP as function of the temperature lift increasing with rising target temperatures [4]. The level of COP is constrained by the Carnot COP as the ideal comparison process. It is therefore particularly important to improve integration efficiency. Second law efficiency summarises all losses in a heat pump cycle fulfilling any process requirements. The better the thermodynamic state changes in the heat pump cycle match the temperature-load requirements of the heat sink or heat source, the higher the second law efficiency [5]. Therefore, in-depth knowledge of the process requirements on the one hand and the adaptation of heat pump concepts on the other is essential.

* Corresponding author. Tel.: +49 5251 60 4138
*E-mail address:* florian.schlosser@upb.de

Kreitlein [6] classified manufacturing processes and distinguished between drying, thermal activation and thermal separation processes. The energy demand is primarily determined by the mass and specific heat capacity of a substance that is heated or cooled from one temperature level to another. Naumann et al. [7] introduced a loss term that primarily accounts for transmission heat losses across the surface of the system, highlighting the relevance of including such effects in a comprehensive modelling approach. While the fundamental principles for estimating thermal energy demand are well known, current models are typically limited to specific unit operations or individual process steps. A generalizable and scalable energy demand building block model that systematically incorporates both basic thermodynamic requirements and process-related losses across multiple industrial thermal processes has not yet been established.

Andersen et al. [8] investigated 16 refrigerants in 10 heat pump cycles under various temperature conditions with the aim of optimal adaptation to a wide range of temperature demands without any specific reference to a process. Transcritical heat pumps are especially well-suited for applications that involve significant temperature changes on the heat sink side, such as in drying processes [9]. According to Mateu-Royo et al. [10], two-stage cascade systems are appropriate for applications requiring temperature lifts exceeding 60 K, whereas single-stage cycles incorporating economizers and parallel compression are more efficient for lifts below 60 K. However, a generalizable framework that systematically links industrial temperature-load profiles with optimal HTHP configurations across multiple processes is still lacking in current literature.

To identify suitable integration points for heat pumps within industrial processes, pinch analysis offers a graphical method – namely, the Grand Composite Curve (GCC) – which enables the determination of target values for appropriately sizing heat pump heating and cooling capacities, along with the associated temperature levels. The correct integration of heat pumps based on pinch analysis was first introduced by Townsend and Linnhoff [11]. Their guideline specifies that the heat pump should extract heat exclusively from below the pinch point and deliver it above. If this integration rule is not followed, the system may experience an increase cooling load due to the heat pump's electricity consumption, without achieving any reduction in heating demand. The COP curve, which facilitates the integration of heat pumps in batch processes, was introduced by Stampfli et al. [12]. Process-specific integration concepts have been developed based on this approach for a range of industrial case studies, including applications in meat and dairy processing, metal treatment, electroplating, paper production, sterilization and manufacturing lines, as summarized by Schlosser et al.[13]. Schlosser et al. [14] utilized the regression models provided by Jesper et al. [15] to estimate the performance of heat pumps available on the market at temperatures up to 160 °C. Although pinch analysis and the GCC have proven effective in identifying heat pump integration points, most existing case studies rely on idealized process conditions or case-specific implementations. A generalized method that systematically determines suitable integration points for HTHPs based on a structured representation of process heat demand is still lacking.

The objective of this paper is to develop and present a generic model and framework to calculate the energy demand of various industrial thermal processes. The aim is to facilitate the integration of heat pump into processes such as distillation, sterilization, cooking, drying, galvanization and pasteurization, targeting suitable integration points and determining the most efficient heat pump concepts. To achieve this, it is necessary to model the process requirements and represent them using the GCC, so they can be aligned with the change of states and performance characteristics of heat pump cycles. Based on that, the framework focuses on key process parameters to derive energy demand and identify the optimal heat pump cycle, refrigerant, size and integration point.

## 2. Approach

In this section, the methods used to develop energy demand models and to identify potentials of heat pump integration are outlined. It includes a description of the selected industrial processes, the modelling approach and the thermodynamic and process parameters applied in the analysis.

### *2.1. Classification of industrial thermal processes*

Industrial thermal processes encompass a wide range of applications where heat is used to induce physical or chemical changes in materials. In order to systematically assess energy demand and identify potentials for heat pump integration, a classification framework is required that captures the diversity of relevant process types across industry sectors. The hierarchical structure of industrial thermal processes is illustrated in Figure 1. Accordingly, thermal processes are classified into four main process types based on their dominant physical principles and heat transfer mechanisms: drying, thermal activation of solid products, thermal activation of fluids and thermal separation. Each process is further subdivided into subcategories and specific industrial processes. The classification reflects not only the type of thermal operation, but also the typical application contexts and the nature of the processed products.

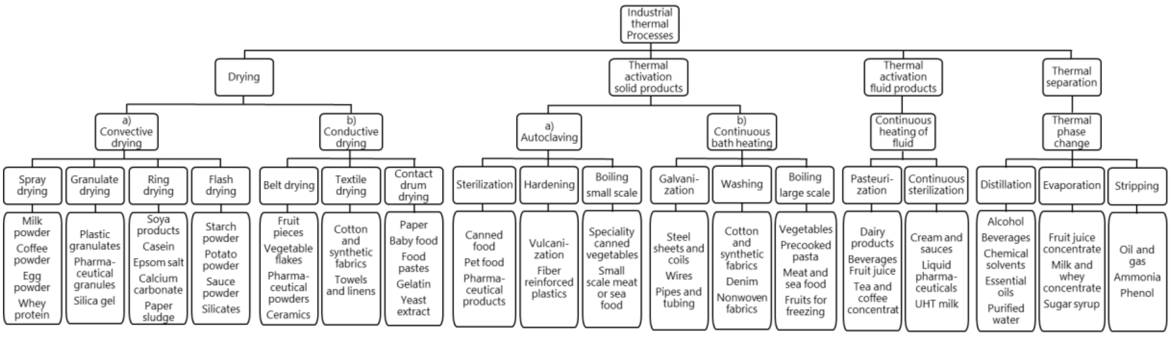


Figure 1. Classification of Industrial Thermal Processes

For instance, the main process type drying includes the categories convective drying and conductive drying. Convective drying comprises processes such as spray drying, granulate drying, ring drying and flash drying, which are typically used for powder or particle-based products. In contrast, conductive drying includes belt drying, textile drying and contact drum drying, commonly applied in sheet-based or textile processing. The process type thermal activation of solid products is divided into autoclaving, including applications like sterilization, hardening and small-scale boiling, and continuous bath heating, which covers galvanization, washing and large-scale boiling operations. The third category, thermal activation of fluid products, includes continuous heating processes such as pasteurization and continuous sterilization, often found in food and beverage industries. Finally, thermal separation includes operations based on thermal phase change, such as distillation, evaporation and stripping, which are prevalent in chemical processing and purification systems. At the lowest level of the hierarchy, each specific process is associated with example product types to contextualize the classification and support subsequent modelling steps. The classification provides the structural basis for the development of generic process models and the identification of thermal integration opportunities, as detailed in the following sections.

### *2.2. Generic Process Energy Demand Modelling*

This section outlines the methodological framework used to develop generic energy demand models for industrial thermal processes. By abstracting representative thermal processes into simplified energy models, the approach enables a scalable and comparative analysis across different sectors and applications. The modelling is based on thermodynamic principles and standardized process assumptions, focusing on relevant parameters such as temperature, mass flows and enthalpy changes. The subsections present the thermodynamic modelling assumptions, describe the classification of industrial thermal processes and detail the development of generic energy demand models for each process type. All energy demand models in this study are based on the First Law of Thermodynamics for open systems, which describe the conservation of energy including mass and heat flows as shown by Eq. (1). In addition to the energy balance, the modelling approach fundamentally relies on the principle of mass conservation, expressed through the mass balance equation, shown in Eq. (2), which ensures that mass flow rates entering and leaving the control volume are accurately accounted for. Together, these conservation laws form the foundation for representing the thermal and material changes within industrial processes. To simplify the modelling approach and focus on thermal energy flows, the following assumptions are applied: No mechanical work is performed; Kinetic and potential energy contributions are neglected; Steady-state conditions are assumed; Homogeneous temperature distribution; Based on these assumptions, the equation is reduced to a steady-state enthalpy balance between incoming and outgoing mass and heat streams. In its simplified form the energy balance for a control volume is written as:

$$\frac{dE}{dt} = \sum \dot{Q}_{in} - \sum \dot{Q}_{out} - \sum \dot{Q}_{loss} + \sum \dot{m}_{in} \cdot h_{in} - \sum \dot{m}_{out} \cdot h_{out} \qquad (1)$$

$$\sum \dot{m}_{in} = \sum \dot{m}_{out} \qquad (2)$$

The generic energy demand models developed here focus on the minimum thermodynamic energy required to drive the specific thermal transitions, as well as characteristic process losses such as thermal dissipation or heat exchanger inefficiencies. These simplified models provide a scalable framework to evaluate different process types based on representative operating conditions. The following subsections outline the modelling approach for each process type, highlighting required input parameters and relevant assumptions.

*2.2.1. Drying*

According to Figure 1, a distinction can be made between convective and conductive dryers. While air serves as the heating medium in convective dryers (see Figure 2 (a)), steam is used in conductive dryers (see Figure 2 (b)). In both dryers, the moist, warm exhaust air can then be used as a heat source. Convective drying processes involve the removal of moisture from a product by means of a heated air stream $\dot{m}_{h,air,i}$ that flows over or through the material. The drying air (cf. Eq. (4)) is first conditioned to a specific desired drying temperature ($T_1$) from a defined initial temperature ($T_0$), often using ambient air as the starting condition. The energy demand needed for the heating is calculated with Eq. (3). This air stream enables drying under approximately isenthalpic conditions, meaning that the total enthalpy of the air remains constant throughout the drying process minus transmission heat losses via the surface of the dryer $(h_1 = h_2 + q_{loss})$ [16]. This is the case because the energy required for the evaporation of moisture from atomized droplets is almost entirely supplied by the thermal energy of the incoming air. As air cools down due to heat transfer to the droplets, water simultaneously evaporates, consuming this heat. These opposing effects balance each other, resulting in minimal change of the total enthalpy of the air-vapor mixture.

$$\dot{Q}_{heating,convective} = \dot{m}_{h,air}(x_1) \cdot (h_1\,(T_1, x_1) - h_0\,(T_0, x_1)) \tag{3}$$

$$\dot{m}_{h,air} = \dot{m}_{air} \cdot (1 + x_i) \tag{4}$$

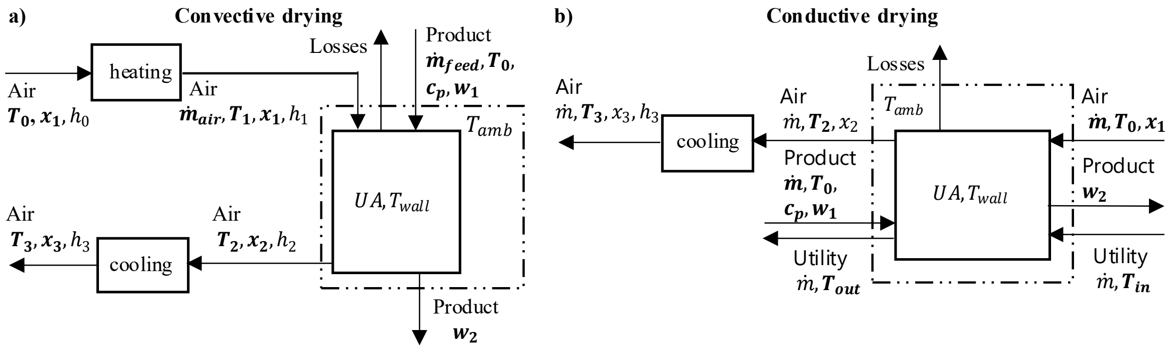


Figure 2. Schematic (a) convective and (b) conductive drying process

In both dryer types, an air stream is used to transfer the vapor away from a product flow ($\dot{m}_{feed}$). The removed water can be calculated with Eq. (5). The outlet air humidity ($x_2$) can be calculated like on convective drying with Eq. (6). As a result of moisture transfer from the product to the air, the outlet humidity ($x_2$) increases while the air temperature ($T_2$) typically decreases. This simplification of quasi-isenthalpic behavior enables the calculation of the outlet conditions as shown in Eq. (7).

$$\dot{m}_{H_2O,\,removed} = \dot{m}_{feed} \cdot (w_1 - w_2) \tag{5}$$

$$x_2 = x_1 + \frac{\dot{m}_{H_2O,\,removed}}{\dot{m}_{air}} \tag{6}$$

$$T_2 = \frac{\dot{m}_{h,air}(x_1) \cdot h_1\,(T_1, x_1) - \dot{m}_{feed} \cdot c_{p,feed} \cdot (T_v - T_0) - U \cdot A \cdot (T_{wall} - T_{amb})}{\dot{m}_{h,air}(x_2) \cdot (c_{p,air} + x_2 \cdot c_{p,v})} - \frac{x_2 \cdot h_v}{(c_{p,air} + x_2 \cdot c_{p,v})} \tag{7}$$

The heat source of the outlet air consists of the 'sensible' cooling down to the dew point temperature, followed by the 'latent' cooling due to condensation as the air is further cooled to the final temperature $T_3$. These calculations are shown in the equations Eq. (8) to (10).

$$\dot{Q}_{sensible} = \dot{m}_{h,air}(x_2) \cdot (h_2(T_2, x_2) - h_{dew}(x_2)) \tag{8}$$

$$\dot{Q}_{latent} = \dot{m}_{h,air}(x_2) \cdot h_{dew}(x_2) - \dot{m}_{h,air}(x_3) \cdot h_{dew}(T_3) \tag{9}$$

$$\dot{Q}_{exhaust\ air} = \dot{Q}_{dew} + \dot{Q}_{latent} \tag{10}$$

In conductive drying (cf. Figure 2 (b)), heat is transferred directly from a heated surface to the wet product through conduction. In contrast to convective drying, no air stream is used to supply the drying energy; instead, the product is in direct contact with a heated surface, such as a plate, drum or belt, which provides the necessary thermal input for moisture evaporation. The drying process typically occurs under quasi-steady state conditions and is driven by the temperature gradient between the hot surface and the product. Moisture evaporates at the product surface, and depending on the system configuration, the resulting vapor is removed either by forced convection or by evacuation under reduced pressure. The energy required for conductive drying (Eq. (14)) is determined by calculating the heat necessary to raise the temperature of the wet product and the transport air to the evaporation temperature $T_v$, like shown in Eq. (11), to evaporate the required moisture as shown in Eq. (12) and to compensate the heat losses via the surface of the dryer (cf. Eq. (13)).

$$\dot{Q}_{sensible} = (\dot{m}_{feed} \cdot c_{p,feed} + \dot{m}_{h,air}(x_1) \cdot (c_{p,air} + x_1 \cdot c_{p,v})) \cdot (T_v - T_0) \tag{11}$$

$$\dot{Q}_{latent} = \dot{m}_{feed} \cdot (w_1 - w_2) \cdot h_v \tag{12}$$

$$\dot{Q}_{loss} = U \cdot A \cdot (T_{wall} - T_{amb}) \tag{13}$$

$$\dot{Q}_{heating,conductive} = \dot{Q}_{sensible} + \dot{Q}_{latent} + \dot{Q}_{loss} \tag{14}$$

Table 1. Required parameters and variables for modelling of drying processes

| (a) Convective drying | (b) Conductive drying |
|---|---|
| Mass flow rate $\dot{m}_{feed}$, specific heat capacity $c_{p,feed}$, $w_1$ and final $w_2$ moisture content of the feed | |
| Mass flow rate dry $\dot{m}_{air}$, initial temperature $T_0$, drying air temperature $T_1$, absolute humidity $x_i$ of drying air, specific heat capacity of air $c_{p,air}$ and vapor $c_{p,v}$ and evaporation enthalpy $h_v$ | |
| | Evaporation temperature $T_v$ |
| $UA$-values of heat transfer areas; external wall temperature $T_{wall}$, ambient temperature $T_{amb}$ | |

### *2.2.2. Thermal activation of solid products*

Essentially, a distinction is made between two overarching processes for this process group: batch autoclaving and continuous bath heating. Batch heating processes are frequently used in the sterilization of packaged products, typically within autoclaves. The process consists of three distinct phases: heating, holding and cooling, during which the product follows a defined temperature-time profile. Continuous thermal activation processes, such as those used in galvanization or textile treatment baths, involve maintaining a stationary fluid medium at a defined setpoint temperature. In contrast to batch processes, the energy demand in steady state arises not from heating up the fluid from ambient conditions, but for two main purposes: thermal losses to the environment and heat absorbed by the product as it is immersed in the bath. Figure 3 illustrates the system configuration of both processes.

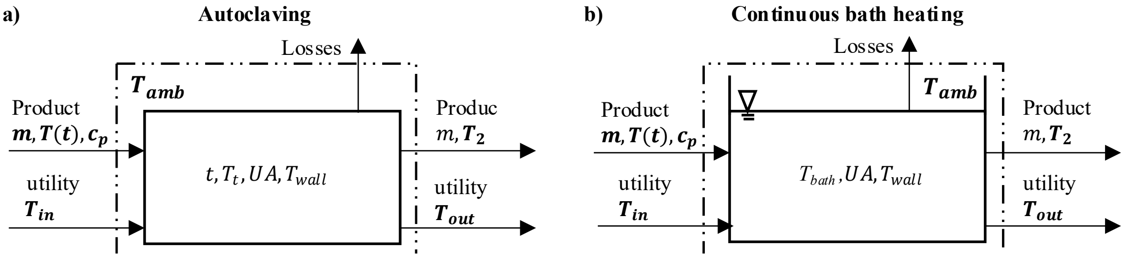


Figure 3. Energy and mass balance around (a) autoclaving and (b) continuous bath heating processes

The energy demand for autoclaving (cf. Figure 3 (a)) is calculated based on the total thermal mass that must be heated and cooled including the product, packaging and autoclave. It is the sum of each component, where $m$ is the mass and $c_p$ the specific heat capacity. The heating demand and cooling demand are calculated using Eq. (15). To calculate the heating and cooling demands, the respective process durations $t_i$ and the start and target temperatures need to be considered for heating and cooling phase. During holding phase, only the second term of heat losses need to be applied. During the cooling phase, the sign of the loss term changes, reducing the cooling demand.

$$\dot{Q}_i(t) = \sum_i m_i \cdot c_{p,i} \cdot \frac{dT(t)}{dt} \pm U \cdot A \cdot (T(t) - T_{amb}) \tag{15}$$

For continuous bath heating (cf. Figure 3 (b)), each product, typically at ambient temperature, is dipped into the heated bath and must be brought to thermal equilibrium with the fluid. This energy must be continuously supplied to offset the thermal load introduced by product immersion and to ensure stable bath operation. In addition, thermal losses to the surroundings, which occur through bath walls and bath cover, are estimated.

Table 2. Required parameters and variables for modelling of processes for thermal activation of solid products

| (a) Autoclaving | (b) Continuous bath heating |
|---|---|
| Mass $m$ of product, packaging and autoclave | Mass $m$ of product |
| Specific heat capacities $c_p$ of each mass | Specific heat capacities $c_p$ of product |
| Actual product temperature $T(t)$, initial product temperature $T_1$ and target temperatures $T_t$ | Actual product temperature $T(t)$, initial product temperature $T_1$ and target temperatures $T_{bath}$ |
| Process time $t$ (heating, holding and cooling phases) | Process time $t$ |
| Inlet temperature $T_{in}$ of the utility stream (e.g. steam, hot water, cooling water) | Inlet temperature $T_{in}$ of the utility stream (e.g. steam, hot water) |
| *UA*-values of heat transferring areas, ambient temperature $T_{amb}$ | |

*2.2.3. Continuous heating of fluids:*

Figure 4 illustrates the process flow, of continuous heating of fluids such as pasteurization. The primary thermal load results from the need to heat the product stream from its inlet temperature to the defined pasteurization temperature and subsequently cool it to a desired outlet temperature after the process. In some configurations, the pasteurization time is slightly exceeded to ensure thermal safety margins. The required thermal load for heating or cooling during pasteurization is calculated using Eq. (16) and (17).

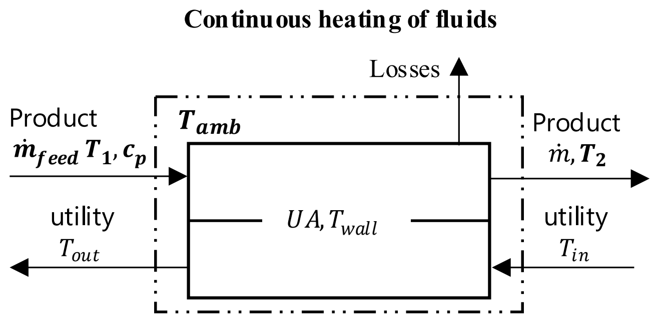


Figure 4. Schematic continuous heating of fluid process

$$\dot{Q}_{heating} = \dot{m}_{feed} \cdot c_{p,feed} \cdot (T_t - T_1) + U \cdot A \cdot (T_{wall} - T_{amb}) \tag{16}$$

$$\dot{Q}_{cooling} = \dot{m}_{feed} \cdot c_{p,feed} \cdot (T_t - T_2) - U \cdot A \cdot (T_{wall} - T_{amb}) \tag{17}$$

Thus, the total thermal energy involved in the process is defined by the combined heating and cooling steps. Since the utility system is not the primary focus, no detailed utility data is required for the energy model.

Table 3. Required parameters and variables for modelling processes for continuous heating of fluids

| Continuous heating of fluids |
|---|
| Mass flow rate $\dot{m}_{feed}$, specific heat capacity $c_{p,feed}$ and inlet temperature $T_{in}$ of the fluid product |
| e.g. pasteurization temperature $T_t = T_{pasteur}$ |
| $UA$-values of heat transferring areas, external wall temperature $T_{wall}$, ambient temperature $T_{amb}$ |
| Outlet temperature after cooling $T_2$ |

*2.2.4. Thermal separation:*

In such processes, a product stream – a liquid mixture with known composition – is partially evaporated, e.g. in a distillation column. The energy demand is primarily driven by two components; the sensible heat required to raise the product stream to boiling temperature and the latent heat needed to evaporate the low-boiling component from the mixture (cf. Figure 5). The heating load is typically supplied by steam. To model the energy demand, the inlet and outlet temperatures of this steam must be known, as well as the latent heat of vaporization. After separation, the two product streams – residual product and distillate – are cooled down if necessary. The energy required to heat the incoming mixture to the boiling point and evaporate the component with the lower boiling point is calculated according to Eq. (18). The energy removed during cooling and condensation is calculated by Eq. (19).

$$\dot{Q}_{heating} = \dot{m}_{feed} \cdot (c_{p,feed} \cdot (T_v - T_1) + w \cdot h_v) + U \cdot A \cdot (T_{wall} - T_{amb}) \tag{18}$$

$$\dot{Q}_{cooling} = \dot{m}_{feed} \cdot (w \cdot (h_v + c_{p,1} \cdot (T_v - T_2)) + (1 - w) \cdot c_{p,2} \cdot (T_v - T_2))) - U \cdot A \cdot (T_{wall} - T_{amb}) \tag{19}$$

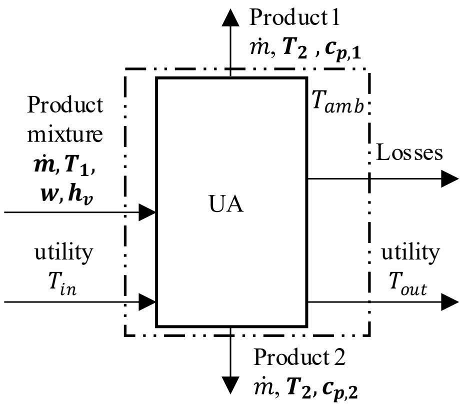


Figure 5. Schematic thermal separation process

Table 4. Required parameters and variables for modelling processes for thermal separation

| Thermal separation |
|---|
| Mass flow rate $\dot{m}_{feed}$, specific heat capacity $c_{p,1}$, $c_{p,2}$, mass fraction $w$ as well as inlet and outlet temperature $T_1$ and $T_2$ of the feed stream and the resulting products |
| Boiling temperature $T_v$, latent heat of $h_v$ of evaporated component |
| $UA$-values of heat transferring areas, external wall temperature $T_{wall}$,ambient temperature $T_{amb}$ |
| Inlet temperature $T_{in}$ of the utility stream (e.g. steam, cooling water) |

*2.3. Targeting of Process-Integrated Heat Pump Concepts*

To identify integration points for heat pumps in industrial processes, a systematic targeting workflow following Figure 6 is applied. This methodology combines generic energy demand modelling, pinch analysis and heat pump cycle simulation to support the selection and optimization of heat pump integration concepts. It provides a structured method to assess technical feasibility across different process types and operating conditions.

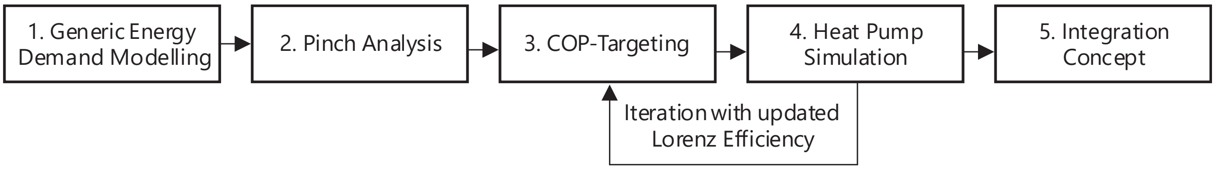


Figure 6. Workflow diagram of targeting method

To systematically identify viable integration points for HTHPs in industrial thermal systems, pinch analysis is applied to the outputs of the generic energy demand models developed for each thermal process type. These models provide representative heating and cooling loads along with associated temperature levels, enabling process-level targeting heat pump integration opportunities without high measurement efforts. The GCC is used as the primary tool for identifying suitable integration points. For each process, the GCC represents the net thermal surplus or deficit across temperature intervals. In this work the targeting method of Schlosser et al. [4] based on the Lorenz-COP according to Eq. (20) with a second law efficiency of 0.55 is used [8]. This provides a physics-based upper benchmark for evaluating the feasibility of integration points identified. Figure 7 illustrates how the heat input $\dot{Q}_c$ is determined by iteratively executing Eq. (21) for source temperatures $T_{so}$ starting from pinch temperature until source capacity is equal to the calculated evaporator capacity for given heating capacity $\dot{Q}_h$ and sink target temperature $T_{si}$.

$$COP = \eta_{2nd} \cdot COP_{Lorenz} = \eta_{2nd} \cdot \frac{\overline{T}_{si}}{\overline{T}_{si} - \overline{T}_{so}} \tag{20}$$

$$\dot{Q}_c(T_{si}) = \dot{Q}_h \cdot (1 - \frac{1}{COP_{Lorenz}})^{-1} \tag{21}$$

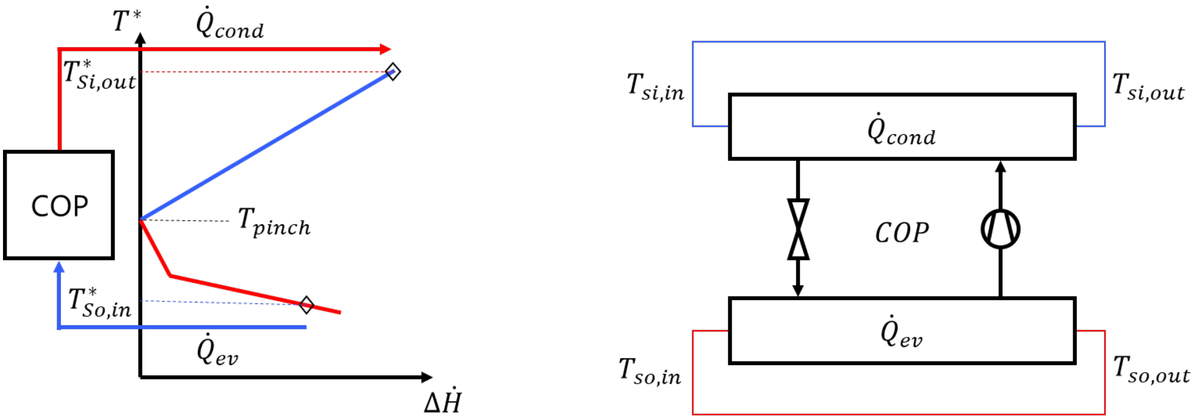


Figure 7. Targeting of integration points using the GCC and schematic illustration of heat pump parameters

In the second step, the assumed second law efficiency is refined using heat pump simulation results. For this study, the results of Andersen et al. [8] are incorporated, which provide the second law efficiencies for 16 refrigerants across 10 different HTHP cycles. Their analysis covers both subcritical and transcritical cycles for source temperatures ranging from 0 °C to 100 °C and temperature lifts from 20 K to 150 K. The refined second law efficiency from simulation is then fed back into the targeting step in an iterative loop, where the updated efficiency is used to reassess the integration point. This approach improves accuracy and robustness of the integration concept, ensuring that both thermodynamic potential and practical constraints are considered. To avoid unnecessary computational effort, the iterative targeting process is terminated once the change in Lorenz efficiency between two successive iterations falls below a defined threshold. In this study, an absolute deviation of 0.01 is used as the convergence criterion. If this condition is met, no further iteration is performed, and the current COP is accepted as the maximal achievable COP based on the corresponding simulation data.

## 3. Results and Discussion

In this section, the results of the energy demand models and the targeting methodology for heat pump integration into various industrial processes are presented and discussed. The analysis includes process-specific thermal energy demands, identified integration points and calculated performance indicators such as COP.

### *3.1. Validation of Process Demand Models*

To verify the accuracy and applicability of the developed energy demand models, a validation was performed by comparing the model outputs with simulation-based models and measurements from literature. Table 5 contains all necessary model parameters from which the necessary material properties can be determined using material databases. One challenge lies in estimating the heat transfer loss factor, which was only available in the literature for the autoclaving example ($UA = 0.208\ kW/K$). In all other examples, both the proposed and the reference modelling approaches calculate the heat demand without considering heat losses. The comparison focuses on key thermal parameters, including overall energy demand and the shape and alignment of GCCs. For example, the corresponding gradients allow the identification of the 'sensitive' and 'latent' heat source ranges in the convective drying example in Figure 8 (a). For a quantitative evaluation, the RMSE and relative deviation is used to assess the differences in enthalpy flow values across the relevant temperature intervals. Across the different process types, the results demonstrate strong alignment between the modelled and reference energy profiles, indicating their suitability for early-stage energy assessments and integration studies.

Table 5. Summary of model parameters and validation results

| Parameter/ Results | Convective drying | Conductive drying | Autoclaving | Bath heating | Fluid heating | Thermal separation |
|---|---|---|---|---|---|---|
| Process Reference | Spray drying [17] | Paper drying [18] | Batch sterilisation [19] | Metal processing [20] | Pasteurization [21] | Distillation [22] |
| Mass flow feed | 3.4 kg/s | 30.0 t/h | 1,114 kg/batch | 6.99 kg/s | 3,135 kg/h | 3.33 kg/s |
| Temporal pattern | continuous | continuous | batch = 3600 s | continuous | continuous | continuous |
| $w_1$ of feed | 0.497 | 0.5 | | | | 0.25 |
| $w_2$ of feed | 0.05 | 0.075 | | | | 0.75 |
| $c_p$ of product 1 | 3.9 kJ/kg K | 2.7 kJ/kg K | 4.0 kJ/kg K | 0.9 kJ/kg K | 3.89 kJ/kg K | 2.353 kJ/kg K |
| $c_p$ of product 2 | | | | | | 2.321 kJ/kg K |
| $h_v$ | 2,256.6 kJ/kg | 2,256.6 kJ/kg | | | | 503 kJ/kg |
| $T_1$ of feed | 15.0 °C | 15.0 °C | 25.0 °C | variable | 4.0 °C | 25.0 °C |
| $T_2$ of product | | | 40.0 °C | variable | 7.0 °C | 30.0 °C |
| Mass flow air: | 55.7 kg/s | 29.5 kg/s | | | | |
| $T_0$ of air/$T_{amb}$: | 15.0 °C | 15.0 °C | 15.0 °C | 15.0 °C | 15.0 °C | 15.0 °C |
| $x_0$ of air: | 6.43 g/kg | 6.43 g/kg | | | | |
| $T_{target}$ | 210.0 °C | 140.0 °C | 121.1 °C | variable | 90.0 °C | 138.0 °C |
| $T_2$ of air | 78.1 °C | 70 °C | | | | |
| $x_2$ of air | 34.35 g/kg | 120 g/kg | | | | |
| $T_3$ of air | 15.0 °C | 25.0 °C | | | | |
| Energy demand | 10,915.8 kW | 9,472.0 kW | 1,546.6 kW | 603.0 kW | 291.3 kW | 1,370.0 kW |
| Reference | 11,134.4 kW | 9,996.3 kW | 1,500.0 kW | 597.0 kW | 278.8 kW | 1,488.0 kW |
| RMSE | 218.6 kW | 524.3 kW | 46.6 kW | 6.0 kW | 12.5 kW | 118.0 kW |
| Rel. deviation | 2 % | 5.5 % | 3.0 % | 1.1 % | 4.3 % | 8.6 % |

### *3.2. Targeting Results*

This section presents the results of the targeting methodology for process-integrated heat pump concepts. For each process type, the thermal energy demands generated by the models were used to derive the GCCs by Pinch Analysis. For targeting integration points according to Eq. (21), an initial Lorenz efficiency value of 0.55 is assumed. Figure 8 shows a multiplot of the targeting results visualized in the GCC.

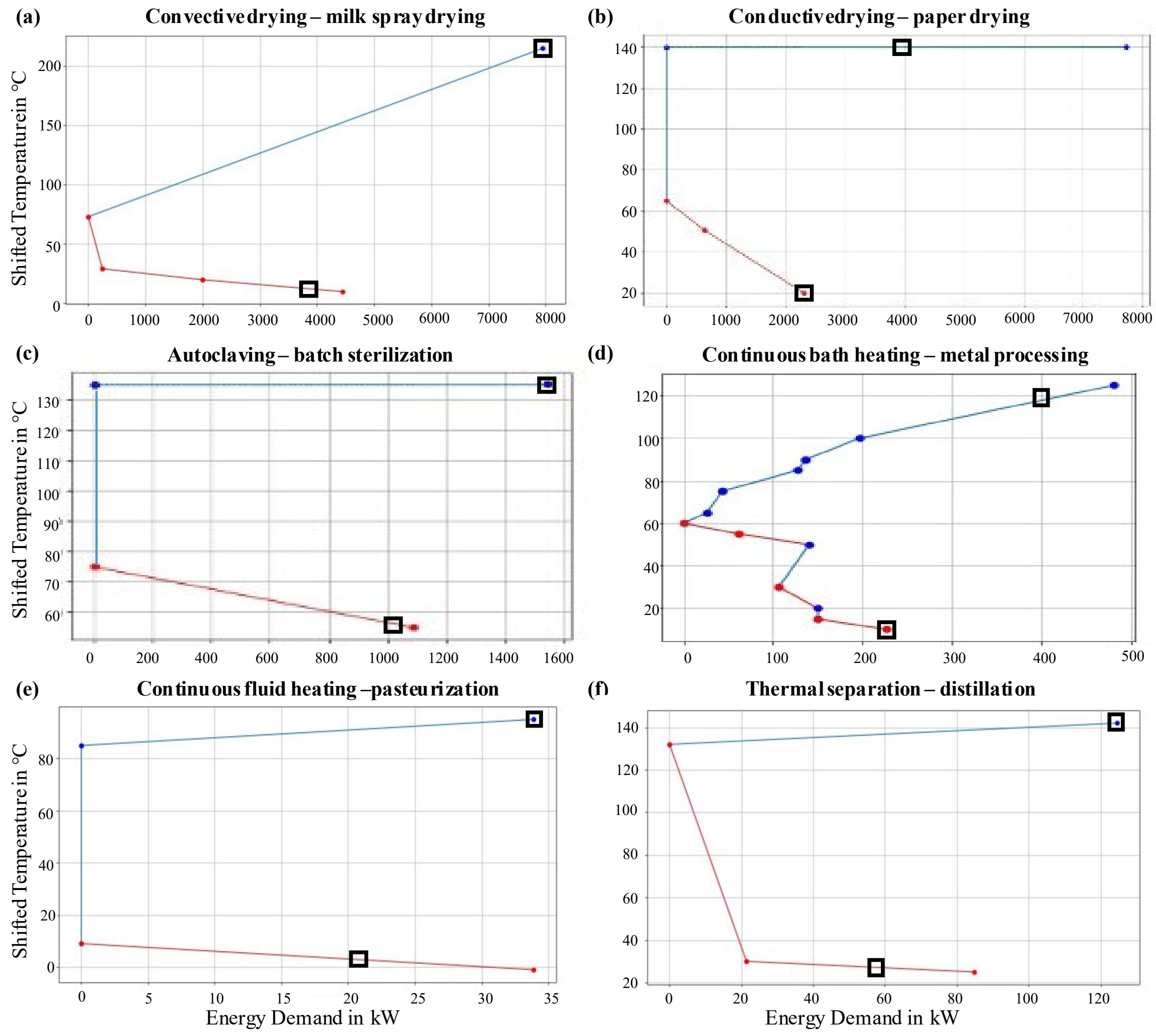


Figure 8. GCCs and integration points (square marker) of targeted HTHP cycle concepts for (a) milk spray drying, (b) paper drying, (c) autoclaving, (d) bath heating, (e) pasteurization and (f) distillation

Table 6 summarizes the targeting results as well as the process-integrated heat pump concepts.The targeting analysis across all process types demonstrates that HTHPs can effectively recover waste heat and upgrade it to meet process heat demands. Depending on the required temperature lifts and the shape of the GCC, both single stage and cascade heat pump cycles were found to be suitable, with final COP values ranging from 1.86 in distillation to 3.15 in batch sterilization. For the spray drying process with its large temperature glide, a single staged transcritical $CO_2$-based cycle with COP of 1.93 is suitable. In contrast, the paper drying process involved a partial heat sink coverage and a small temperature glide, which required a cascade system using isopentane and water. The iterative approach led to a final COP of 2.50 and a converged Lorenz efficiency of 0.59, highlighting the value of the methodology for optimizing system configuration. In both thermal activation cases, the integration points occurred at sink temperatures above 110 °C, demanding cascade cycles for the high temperature lifts and small temperature glides. In contrast, complete coverage cannot be achieved for the continuous bath heating example. For batch sterilization, the heat pump configuration provided full substitution of external steam during the sterilization phase. However, since the heat sink and the heat source are not concurrent, thermal energy storage systems are required to buffer the heat and enable effective integration of heat pump. The pasteurization and distillation processes both exhibited strong internal heat recovery, leading to relatively low net heat demands in the GCC. Despite this, the remaining heating requirement could be effectively met by heat pump systems. In both cases, a dual-stage cascade was selected, enabling efficient operation even with low source temperatures and high sink temperatures. These configurations demonstrate the versatility of HTHPs in processes with both low- and high-temperature constraints.

Table 6. Summary of targeting results for process-integrated HTHP concepts

| Process type | Process example | COP | $\eta_{2nd}$ | HTHP cycle concept | Refrigerants |
|---|---|---|---|---|---|
| Convective drying | Spray drying | 1.93 | 0.55 | Transcritical single-stage cycle | R-744 |
| Conductive drying | Paper drying | 2.50 | 0.59 | Cascade cycle with IHX (bottom) | R-601a, R-718 |
| Autoclaving | Batch sterilization | 3.15 | 0.55 | Cascade cycle with IHX (bottom) | R-602, R-718 |
| Continuous bath heating | Bath heating | 2.56 | 0.65 | Cascade cycle with IHX (both) | R-600, R-601a |
| Continuous fluid heating | Pasteurization | 2.68 | 0.6 | Cascade cycle with IHX (both) | R-600, R-601a |
| Thermal separation | Distillation | 1.86 | 0.5 | Cascade cycle with IHX (both) | R-600, R-601a |

The iterative COP refinement method based on Lorenz efficiency proved to be a useful tool for convergence assessment and cycle type selection. In processes with steep or narrow temperature glides, multiple iterations were sometimes needed to reach convergence and optimal design. These findings emphasize that accurate estimation of both heat source/sink characteristics and thermodynamic performance is essential to avoid under- or oversizing of the heat pump system. Moreover, while the current study leverages literature-based heat pump simulation data to refine COP estimates, future work should prioritize conducting dedicated cycle simulations tailored to the process-specific energy demand. This approach would enhance the accuracy of performance predictions and allow for more precise optimization of cycle configurations and refrigerant selection, ultimately improving the reliability of the integration assessments.

While the results demonstrate strong potential for HTHP integration, several limitations must be noted. The models do not account for transient effects, control system dynamics or equipment fouling, which may impact real-world performance. The general assumptions regarding heat loss terms and homogeneous temperature distribution also lead to deviations between real and model behavior. However, the moderate RMSE values suggest sufficient accuracy for an initial feasibility assessment. Future research should extend the methodology to dynamic process modelling, include techno-economic assessments and prioritize dedicated heat pump cycle simulations based to the generic energy demand models developed here to enhance performance accuracy.

## 4. Conclusion

This study presents a methodological framework for assessing the integration potential of high-temperature heat pumps across various industrial thermal processes, supported by validated generic energy demand models. The validation against reference data from literature and case studies demonstrated that the models reliably capture process-specific thermal energy demands, enabling accurate early-stage evaluations of heat integration opportunities without high measurement efforts. The targeting methodology revealed that HTHPs can effectively recover and upgrade waste heat streams, with feasible configurations ranging from single cycles for lower temperature lifts over transcritical operating heat pump for large temperature glides to advanced cascade systems for processes demanding high temperature lifts.

Future work should focus on advancing the simulation of heat pump cycles directly tied to the developed generic energy demand models, moving beyond literature-based data to improve the fidelity and applicability of performance predictions. Additionally, incorporating dynamic process modelling and techno-economic assessment will be crucial steps for practical application of stakeholders accelerating market uptake of HTHPs.

## Acknowledgements

The work is funded by Federal Ministry for Economic Affairs and Energy Germany – BMWE (HeatTransPlan, FKZ 03EN2109A).

## References

[1] Zühlsdorf, B., Andersen, M. P., Tammone, C. et.al. Industrial High-Temperature Heat Pumps. Task 1 – Technologies: Yearly Report 2025 2025. https://doi.org/10.23697/9b7b-sz34.

[2] Annex 48. Industrial Heat Pumps - IEA HPT TCP ANNEX 48: Map of case studies. [June 04, 2020]; Available from: https://waermepumpe-izw.de/karte-europa.

[3] Boer R de, Marina A, Zühlsdorf B, Arpagaus C, Bantle M, Wilk V et al. Strengthening Industrial Heat Pump Innovation: Decarbonizing Industrial Heat. White Paper 2020.

[4] Schlosser F, Zysk S, Walmsley TG, Kong L, Zühlsdorf B, Meschede H. Break-even of high-temperature heat pump integration for milk spray drying. Energy Conversion and Management 2023;291:117304. https://doi.org/10.1016/j.enconman.2023.117304.

[5] Zühlsdorf B, Jensen JK, Cignitti S, Madsen C, Elmegaard B. Analysis of temperature glide matching of heat pumps with zeotropic working fluid mixtures for different temperature glides. Energy 2018;153:650–60. https://doi.org/10.1016/j.energy.2018.04.048.

[6] Kreitlein S. Der grundoperationsspezifische Mindestenergiebedarf als Referenzwert zur Bewertung der Energieeffizienz in der Produktion [Dissertation]: Friedrich-Alexander-Universität Erlangen-Nürnberg (in German).

[7] Naumann M, Henne K, Ostermann M, Schlosser F, Meschede H. Modular Energy Demand Modeling of Manufacturing Processes for Energy Efficiency Improvement. Procedia CIRP 2025;135:1351–8. https://doi.org/10.1016/j.procir.2025.08.002.

[8] Andersen MP, Zühlsdorf B, Markussen WB, Jensen JK, Elmegaard B. Selection of working fluids and heat pump cycles at high temperatures: Creating a concise technology portfolio. Applied Energy 2024;376:124312. https://doi.org/10.1016/j.apenergy.2024.124312.

[9] Adamson K-M, Walmsley TG, Carson JK, Chen Q, Schlosser F, Kong L et al. High-temperature and transcritical heat pump cycles and advancements: A review. Renewable and Sustainable Energy Reviews 2022;167:112798. https://doi.org/10.1016/j.rser.2022.112798.

[10] Mateu-Royo C, Arpagaus C, Mota-Babiloni A, Navarro-Esbrí J, Bertsch SS. Advanced high temperature heat pump configurations using low GWP refrigerants for industrial waste heat recovery: A comprehensive study. Energy Conversion and Management 2021;229:113752. https://doi.org/10.1016/j.enconman.2020.113752.

[11] Townsend DW, Linnhoff B. Heat and power networks in process design. // Heat and power networks in process design. Part I: Criteria for placement of heat engines and heat pumps in process networks. AIChE J. 1983;29(5):742–8. https://doi.org/10.1002/aic.690290508.

[12] Stampfli JA, Atkins MJ, Olsen DG, Walmsley MRW, Wellig B. Practical heat pump and storage integration into non-continuous processes: A hybrid approach utilizing insight based and nonlinear programming techniques. Energy 2019;182:236–53. https://doi.org/10.1016/j.energy.2019.05.218.

[13] Schlosser F, Arpagaus C, Walmsley TG. Heat Pump Integration by Pinch Analysis for Industrial Applications: A Review. Chemical Engineering Transactions 2019;76:7-12. https://doi.org/10.3303/CET1976002.

[14] Schlosser F, Jesper M, Vogelsang J, Walmsley TG, Arpagaus C, Hesselbach J. Large-scale heat pumps: Applications, performance, economic feasibility and industrial integration. Renewable and Sustainable Energy Reviews 2020;133:110219. https://doi.org/10.1016/j.rser.2020.110219.

[15] Jesper M, Schlosser F, Pag F, Walmsley TG, Schmitt B, Vajen K. Large-scale heat pumps: Uptake and performance modelling of market-available devices. Renewable and Sustainable Energy Reviews 2021;137:110646. https://doi.org/10.1016/j.rser.2020.110646.

[16] Kraume M. Transport processes in process engineering. Berlin, Heidelberg: Springer Berlin Heidelberg; 2020 [in German].

[17] Bühler F, Nguyen T-V, Jensen JK, Holm FM, Elmegaard B. Energy, exergy and advanced exergy analysis of a milk processing factory. Energy 2018;162:576–92. https://doi.org/10.1016/j.energy.2018.08.029.

[18] Ager E. High Temperature Heat Pumps in Paper Drying Processes: A Techno-Economic Analysis. Stockholm; 2023.

[19] Hechelmann R-H, Philipp M, Schumm G, Hesselbach J, Walmsley TG. Energy Efficiency Measures for Batch Retort Sterilization in the Food Processing Industry. Chemical Engineering Transactions 2016;52:163–8. https://doi.org/10.3303/CET1652028.

[20] Schlosser F, Walmsley TG, Lincoln B, Meschede H. Retrofit of a Galvanisation Plant using Advanced Heat Pump Bridge Analysis. Chemical Engineering Transactions 2023;103:319–24. https://doi.org/10.3303/CET23103054.

[21] Landi G, Benedetti M, Sforzini M, Eslami E, Pataro G. Comparative Analysis of Cost, Energy Efficiency, and Environmental Impact of Pulsed Electric Fields and Conventional Thermal Treatment with Integrated Heat Recovery for Fruit Juice Pasteurization. Foods 2025;14(13). https://doi.org/10.3390/foods14132239.

[22] Oppenheimer O, Sørensen E. Comparative energy consumption in batch and continuous distillation. Computers & Chemical Engineering 1997;21:529–34.